Comparison of Computational Fluid Dynamic Simulation of a Stirred Tank with Polyhedral and Tetrahedral Meshes

Zhang, Hegui; Tang, Siyang; Yue, Hairong
School of Chemical Engineering, Sichuan University, Chengdu 610065, P.R. CHINA

Wu, Kejin; Zhu, Yingming
Institute of New Energy and Low-Carbon Technology, Sichuan University, Chengdu 610207, P.R.CHINA

Liu, Changiun*[+]; Liang, Bin[•]; Li, Chun
School of Chemical Engineering, Sichuan University, Chengdu 610065, P.R. CHINA

ABSTRACT: *This work compares the accuracy and calculation efficiency of various tetrahedral and polyhedral meshes in a Computational Fluid Dynamic (CFD) simulation of a stirred tank. The polyhedral mesh was found leading to much fewer mesh cells than the tetrahedral one without missing the calculation accuracy. The CFD numerical simulation results of the polyhedral mesh better agree to the experimental data comparing to the tetrahedral one at the same mesh cell number. In addition, the results of polyhedral mesh were also found to be more accurate than the tetrahedral one which was refined by adaptive meshing based on the velocity gradient.*

KEYWORDS: *Polyhedral; Tetrahedral mesh; Stirred tank; CFD simulation*.

INTRODUCTION

Stirred tanks have been widely used in many fields, such as chemical metallurgy, wastewater treatment, pharmaceutical, biological industry and chemical industry[1,2]. The scale-up of a mechanically agitated tank largely depends on the limited empirical or semi-empirical formulas derived from numerous experiments[3,4]. Understanding the flow field in the whole tank, under operation conditions, is especially important for large scale applications due to its complexity. However, building and running large scale experimental setup is highly time and money -consuming, besides it is not easy to accurately monitor the whole flow field in large scale stirred tanks, according to the current Laser Doppler Velocimetry (LDV) and Particle Image Velocimetry (PIV) techniques. The numerical simulation of an industrial scale stirred tank, using Computational Fluid Dynamic (CFD) method, provides a promising way for better understanding on the flow and mixing in a tank beforehand. Semi-empirical scale up correlation of a stirred tank based solely on the CFD model has been found feasible[5]. However, the CFD simulation of large scale stirred tank is still costly due to huge computational time demand.

The computational mesh is critical for the time required for a CFD simulation. Tetrahedral and hexahedral meshes are most extensively adopted in many CFD simulations with moving parts. Tetrahedral mesh can be used

***** *To whom correspondence should be addressed.*
+ E-mail: liuchangjun@scu.edu.cn
• *Other Address:* Institute of New Energy and Low-Carbon Technology, Sichuan University, Chengdu 610207, P.R.CHINA
1021-9986/2020/4/311-319 *9/$/5.09*

without any restriction due to its simplicity as a volume element. Any geometry of a simulation domain can be theoretically filled with tetrahedrons. Thus, the tetrahedral meshes can be automatically generated easily and quickly with almost all commercial CFD software tools [6]. However, the disadvantage of tetrahedral mesh is the huge mesh number and computational time required to achieve the result with reasonable accuracy. Its computing resources consumption is huge if there are some subtle geometric structures, such as small gaps, long channels, which dramatically increases the mesh number due to its limited stretching capability. Hexahedral meshing has also been tried in CFD simulations with moving parts due to its high accuracy and high computational efficiency [7]. However, meshing of hexahedron is quite difficult particularly for those complex geometries with moving parts. Fewer applications of hexahedral mesh have been found in the simulation of stirred tanks. Mixed mesh of tetrahedron and hexahedron has also been adopted for the simulation of stirred tanks with aim to take advantages of both meshes. Generally, the rotating part with a complex geometry was meshed with tetrahedron while the stationary part was meshed with hexahedron [8-10]. However, this kind of mixed mesh generally has larger errors in the conjunction area due to the discontinuity at their interface. Thus, currently the tetrahedral meshes have been more frequently used in the CFD simulations with moving parts despite its huge computational consumption[11-13].The increase of mesh number is mainly due to the complexity of the impeller in the simulation of stirred tank. Such increase in mesh number leads to high demands on the memory and computing time. Therefore, a mesh with high computational efficiency and accuracy, can be automatically and quickly generated, is desirable.

The polyhedron can also be used in automatic meshing as tetrahedron, which has 1.5 times more neighbors than the tetrahedron one. More neighbors can approximate the gradient better than tetrahedral mesh. *Spiegel et al.* [14] compared polyhedral and tetrahedral meshes in cerebral hemodynamic simulation and the results show that the polyhedral meshes have a better convergence, shorter computation time and higher wall shear stress accuracy compared to the tetrahedral ones. *Diedrichs et al.* [15] found the arbitrary polyhedral cells is applicable in the simulation of crosswind stability of high-speed train under various flow field conditions. *Tritthart et al.* [16] showed that polyhedral meshes have the potential of offering even more accurate simulation results in the recirculation zones of a river than hexahedral meshes. The polyhedral mesh has more faces than the hexahedral mesh, which can lead to more optimal flow directions and the maximum accuracy in a complex flow simulation. [6]. However, how the performance of the polyhedral mesh in the numerical simulation of stirred tank comparing to other meshes is still unclear. This work compares the CFD simulation efficiency and accuracy of various meshes in a numerical simulation of a stirred tank. The results are helpful for large scale stirred tank simulation.

THEORITICAL SECTION

Mathematical model

Governing equations

For the simulations of single-phase flow, the governing equations include continuity and momentum conservation (Navier-Stokes, NS) equations. The equations for incompressible flow are given by:

$$\frac{\partial \rho}{\partial t} + \nabla \cdot (\rho \mathrm{u}) = 0 \tag{1}$$

$$\frac{\partial (\rho u)}{\partial t} + \nabla \cdot (\rho \mathrm{uu}) = -\nabla P + \nabla \cdot (\boldsymbol{\tau}) + \rho g + \boldsymbol{F} \tag{2}$$

Where P is the pressure, $\boldsymbol{F}$ is the external force, the τ is calculated by the formula $\boldsymbol{\tau} = \mu(\nabla u + u^T) - \frac{2}{3}\nabla \cdot uI$, where $\boldsymbol{I}$ is the unit tensor.

Turbulence model

The focus of this work is to understanding difference in mesh forms for stirred tank simulation. The $k-\varepsilon$ turbulence model has been adopted due to its approved robustness and validity in various scales of turbulent flow simulation [7,10,17-19], although some other turbulence models could be a better option for stirred tank simulation[20-22]. The turbulence kinetic energy, k, and its rate of dissipation, ε, in $k-\varepsilon$ model is defined by Eqs. (3) - (6)

$$k = \frac{1}{2}\left[\overline{u_i'^2} + \overline{u_j'^2} + \overline{u_k'^2}\right] \tag{3}$$

and

$$\varepsilon = \frac{\mu_t}{\rho}\overline{\left(\frac{\partial u_i'}{\partial x_j}\right)\left(\frac{\partial u_i'}{\partial x_j}\right)} \tag{4}$$

$$\mu_t = \rho C_\mu \frac{k^2}{\varepsilon} \tag{5}$$

$$C_\mu = 0.09 \tag{6}$$

Where u' is the fluctuation term for velocity, μ_t

is turbulent viscosity. The values of k and ε were calculated from the transport equations:

$$\frac{\partial}{\partial t}(\rho k)+\frac{\partial}{\partial x_i}(\rho k u_i)=\frac{\partial}{\partial x_j}\left[\left(\mu+\frac{\mu_t}{\sigma_k}\right)\frac{\partial k}{\partial x_j}\right]+ \quad (7)$$

$$G_k+G_b-\rho\varepsilon$$

$$\frac{\partial}{\partial t}(\rho \varepsilon)+\frac{\partial}{\partial x_i}(\rho \varepsilon u_i)=\frac{\partial}{\partial x_j}\left[\left(\mu+\frac{\mu_t}{\sigma_\varepsilon}\right)\frac{\partial \varepsilon}{\partial x_j}\right]+ \quad (8)$$

$$G_{1\varepsilon}\frac{\varepsilon}{k}+(G_k+C_{3\varepsilon}G_b)-C_{2\varepsilon}\rho\frac{\varepsilon^2}{k}$$

Here the model constants had the following default values: $C_{1\varepsilon}=1.44$, $C_{2\varepsilon}=1.92$, $C_{3\varepsilon}=\tanh|u_j/u_i|$, $\sigma_\varepsilon=1.3$, $\sigma_k=1.0$.

More details about $k-\varepsilon$ model can be found in reference [23].

Geometry model and meshing

Geometric model

A typical stirred tank equipped with a six-blade standard Rushton turbine and four radial baffles as Fig. 1 shown was set up in CFD simulation. The single-phase flow in a stirred tank with both liquid height (H) and tank diameter (T) of 300 mm were adopted according to the reference [24,25]. An impeller with a diameter(D) of 100 mm (D = T/3) was installed with an off-bottom clearance (C) of T/2. The width of baffle (b) is 0.1 T and the height of each blade (w) is 0.2 D, the width (*l*) and thickness of the blades are 0.25 D and 0.02 D, respectively.

Meshing

The tetrahedral mesh was generated by a commercial software ICEM CFD 18.0 based on the octree method and the meshes are refined in those large velocity gradient areas. The polyhedral mesh was generated from tetrahedral ones in the solver of Fluent 18.0. New edges were created between the face centroid and the centroids of the edges of such face in every faces of a tetrahedral cell (Fig. 2). Then, these new edges are connected to the tetrahedral cell centroid in order to create new faces, which establish the boundaries within the cell. In this way, ANSYS Fluent decomposes a tetrahedral cell into 4 sub-volumes called "duals". Each dual is associated with a node of the original tetrahedron. A polyhedral cell is made up by the duals which share a certain node (Fig.3). More details about the conversion process can be found in Fluent Help Manual [26].

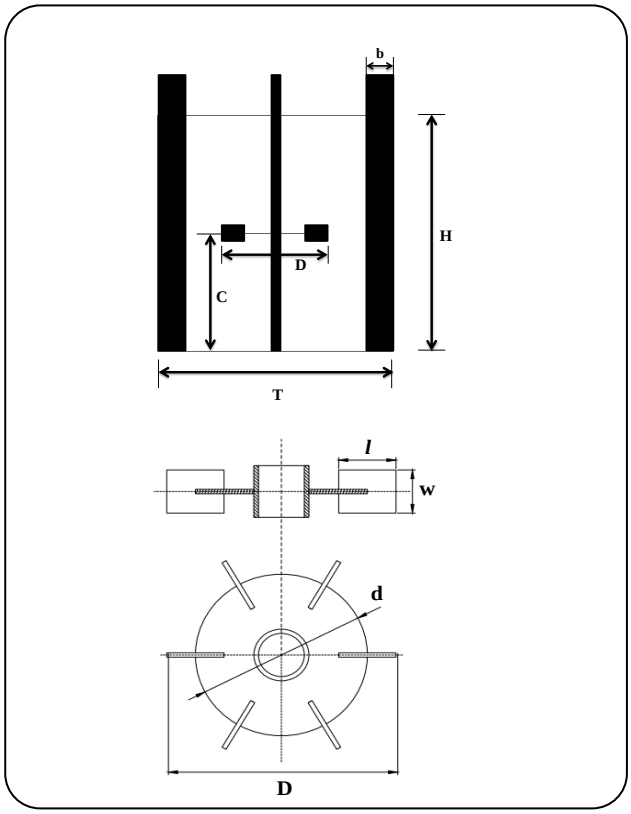

Fig. 1: Schematic view of the stirred tank.

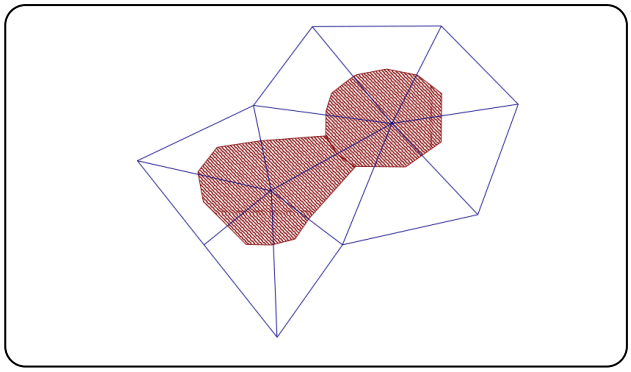

Fig. 2: Connection between edge centroids and face centroids in a tetrahedral cell [26].

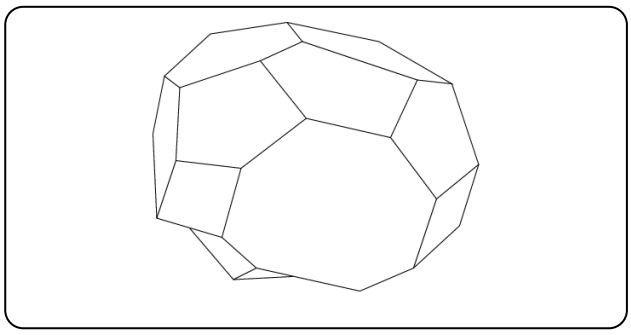

Fig. 3: A polyhedral cell [26].

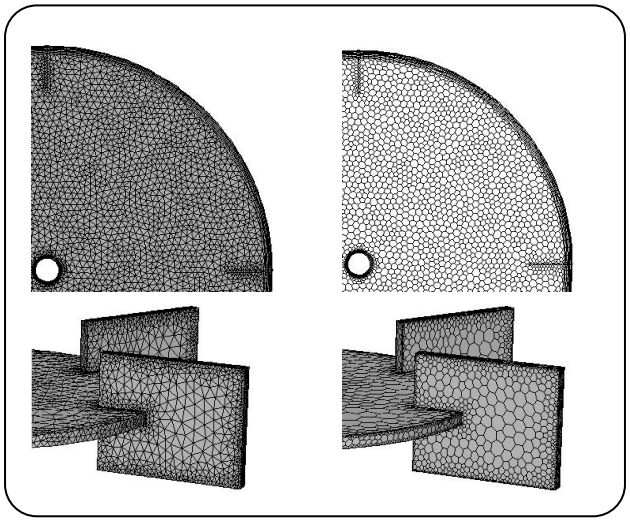

Fig. 4: Views of the computational mesh for stirred tank before and after conversion. left: tetrahedral mesh; right: polyhedral mesh.

In this work, the polyhedral meshes were generated as mentioned above. During the conversion process, only the tetrahedral cells are converted, and the prism layer mesh is not. Fig. 4 shows both tetrahedral and polyhedral meshes of an impeller.

RESULTS AND DISCUSSION

Grid independence

The grid quality is one of the key factors which determines the accuracy of the CFD simulation of a stirred tank. Generally, smaller grid lead to more accurate results at the expense of larger computational demands. However, the small grid of a large industrial scale reactor will result in a huge number of mesh cells. It is known that the mesh shape could significantly affect the simulation consumption and result. Generally, simulation of minimum computational requirements and acceptable accuracy is desirable. Simulations of a stirred tank at an impeller rotation speed of 200 rpm were performed with various numbers of tetrahedral meshes. Fig. 5 compares the axial profiles of non-dimensional axial, radial and tangential velocities derived from mesh numbers of 0.72 million, 1.0 million, 1.56 million and 2.51 million, respectively. The velocities were normalized by blade tip velocity ($U_{tip} = \pi DN, W^* = {}^{U}/_{U_{tip}}$), where N is the rotational speed (s^{-1}). The Y-axes were normalized by the half of blade height (Z*=2z/W) and the radial coordinates were normalized by the radius of impeller ($r^* = {}^{2r}/_{D}$).

Significant difference was observed between the simulation results with the mesh cell number less than 1.0 million. The simulation results of non-dimensional velocities were found consistent as the number of mesh cells increased from 1.0 million to 2.51 million. Thus, a grid cell number of 1.0 million is selected as the mesh cell number criterion for the following simulations.

Comparison of the single-phase flow derived from tetrahedral and polyhedral meshes

The previous tetrahedral mesh, with a cell number of 1.0 million, was transformed into a polyhedral mesh with a cell number of about 0.25 million by the aforementioned method. In another case, the polyhedral meshes were refined for the areas close to the impeller which led to a grid cell number of 0.34 million. The axial profiles of the non-dimensional axial, radial and tangential velocities at impeller rotation speed of 200 rpm were calculated with 1.0 million tetrahedral mesh, 0.25 million and 0.34 million polyhedral mesh respectively. The calculation results were compared to each other as well as to the experimental LDA and PIV results in literatures [24] and [25] (Fig. 6) .

Fig. 6 shows that all simulation results well agree with the experimental observations although the simulation result of the 0.25 million polyhedral mesh showed slightly larger deviation at the vicinity of impeller, particularly the radial and tangential velocities. This is due to the large velocity gradient around the impeller and no enough polyhedral meshes in this area. Refining the vicinity of the impeller with extra polyhedral meshes leads to a grid cell number of 0.34 million. The simulation results with the partly refined polyhedral mesh overlap with the ones from the 1.0 million tetrahedral mesh. Fig. 6 clearly show that the polyhedral mesh leads to more accurate results in stirred tank simulation with less grid cell number than tetrahedral one does. The relative computing time t_{RCT} (Table 1) was adopted to compare the computing performance of different meshes. The relative computing time is defined as $t_{RCT} = t / t_0$, where, t_{RCT} is the relative computing time, t is the computing time of each case, t_0 is the computing time of the 1.0 million tetrahedral mesh case. Table 1 shows that the refined polyhedral mesh requires much less computing time and resources to achieve comparable sound simulation result.

On the other hand, Fig. 7 compares the simulation results of both the tetrahedral and polyhedral meshes

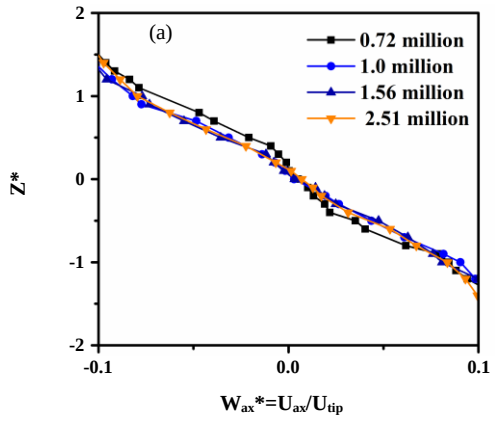

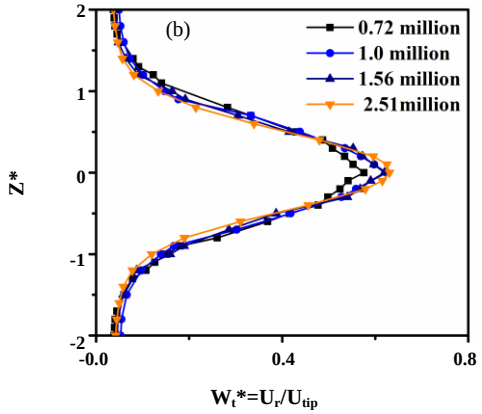

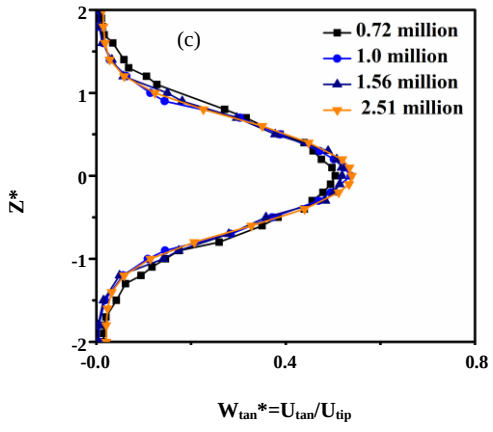

Fig. 5: Axial profiles of non-dimensional average axial, radial and tangential velocities at r=1.2.*

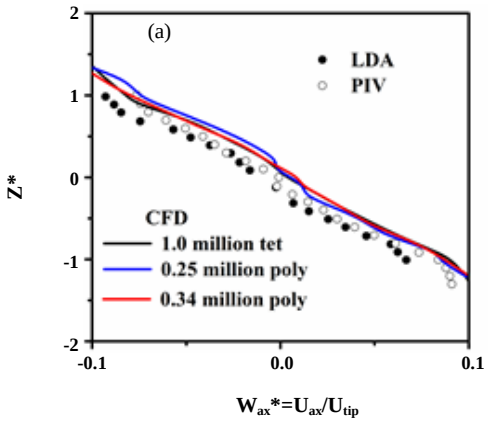

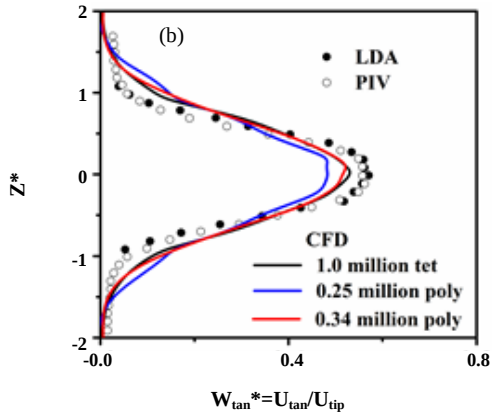

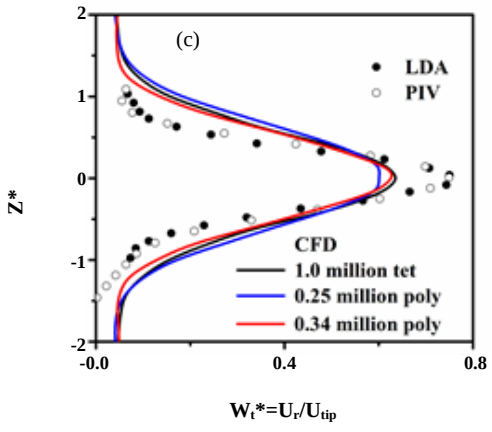

Fig. 6: Axial profiles of non-dimensional average axial (a) and tangential (b) velocities at r=1.2; and non-dimensional average radial velocities at r*=1.05 (c).*

Table 1: The relative computing times of different mesh forms.

Mesh	1.0 million-tet	0.34 million-poly	0.25 million-poly
t_{RCT}	1.0	0.246	0.159

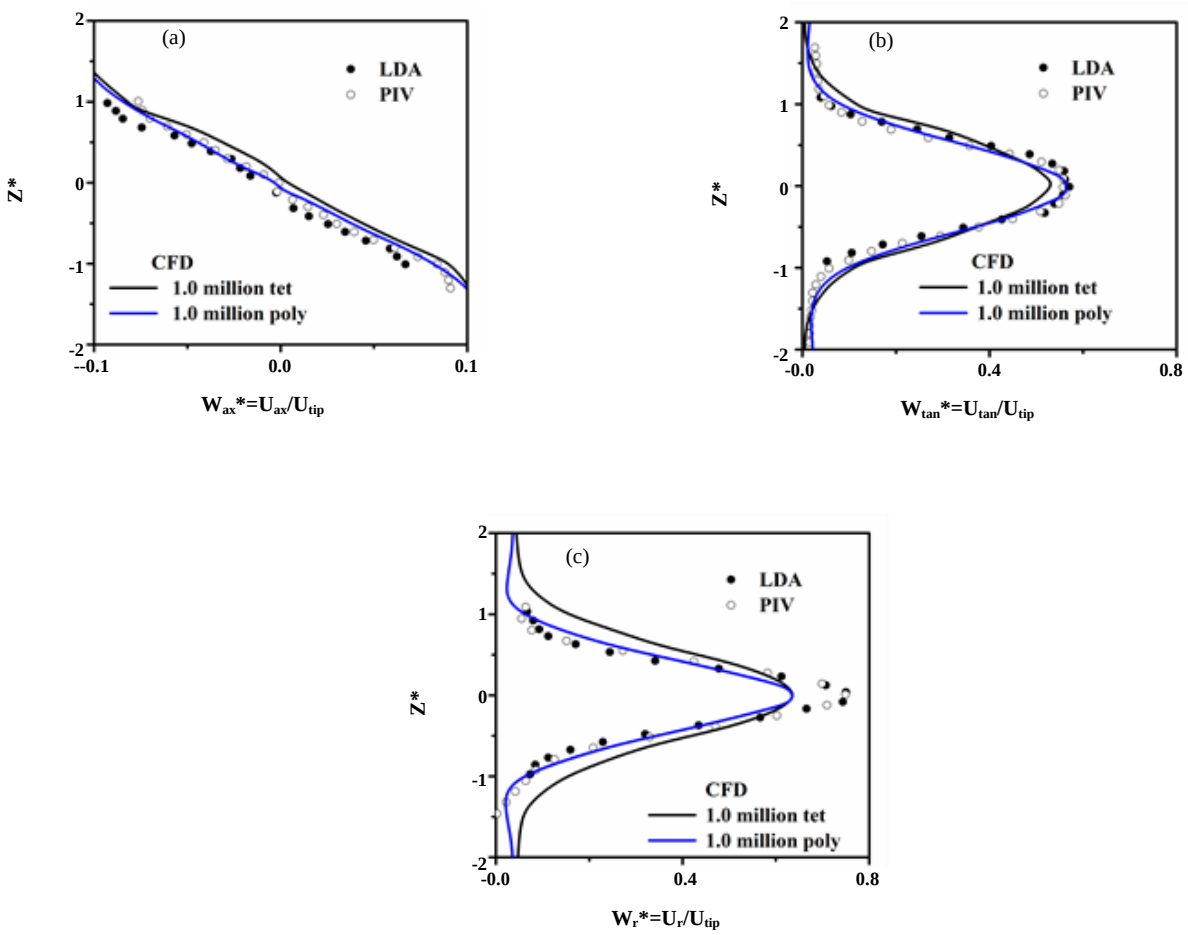

Fig. 7: Axial profiles of non-dimensional average axial (a) and tangential (b) velocities at r*=1.2; and non-dimensional average radial velocities at r*=1.05 (c).

with 1.0 million mesh cells. The 1.0 million polyhedral grid cells led to significant improvement in simulation accuracy. The simulation results better agree with the experimental results. The clouds of the flow field (Fig. 8) and the kinetic energy (Fig. 9) show that the polyhedral mesh led to much smoother clouds than the tetrahedral one. The polyhedral mesh has slightly larger number of mesh nodes than the tetrahedral one, which significantly improve the prediction of high gradient area. This is likely due to the larger number of neighbors for each node in polyhedral meshes than that of the tetrahedral mesh, which can approximate the gradient better. Less numerical diffusion can be achieved since fluxes of momentum in more coordinate directions can be calculated in polyhedral meshes [18]. There are six optimal flow directions which lead to the maximum accuracy for a polyhedron with 12 faces.

Adaptive meshes are increasingly attracting the attention of researchers in CFD simulations since it can improve the simulation quality without completely refining the mesh. This technique can modify the grid size according to the research concern, such as the velocity gradient, value of $Y+$ based on the initial results

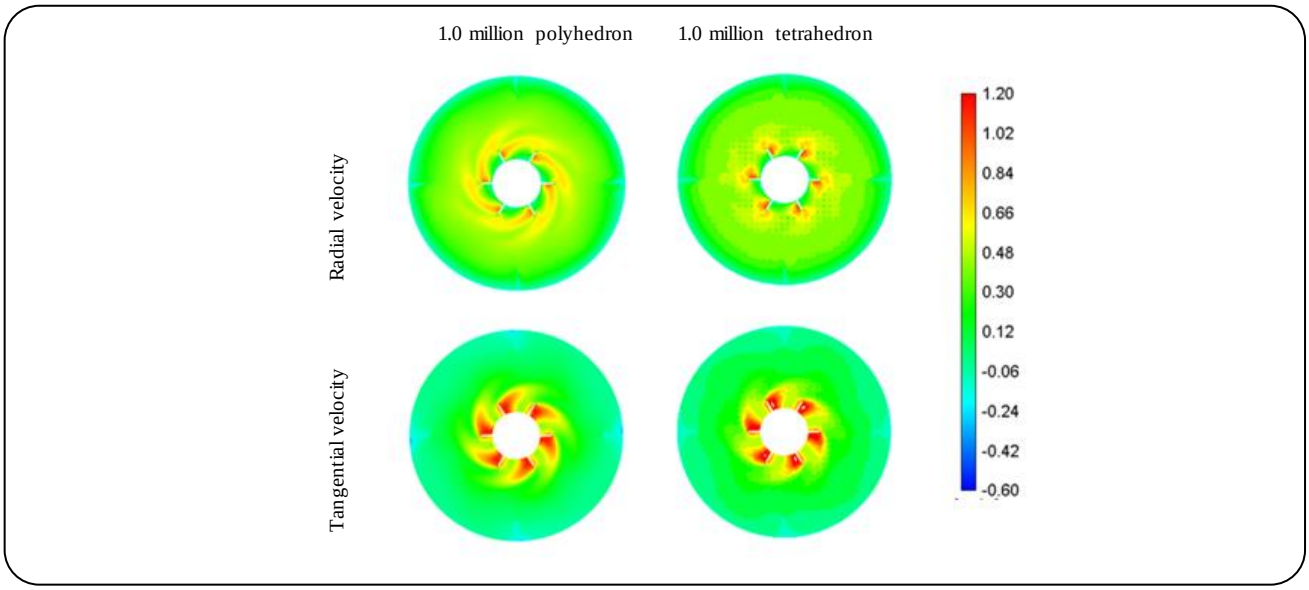

Fig. 8: Predicted radial and tangential velocity from different meshes with similar mesh number on the horizontal axial of the impeller (T=300 mm, 200 rpm).

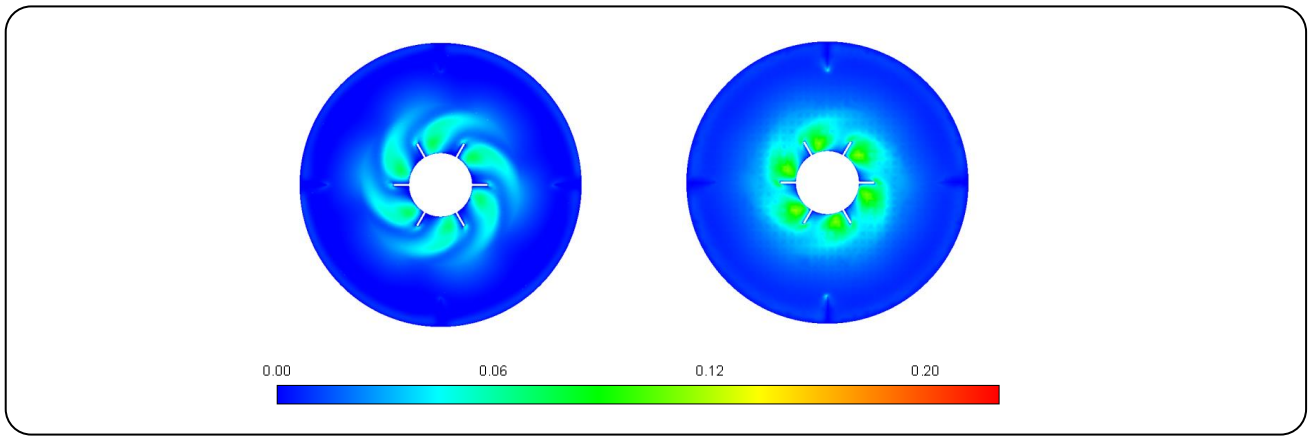

Fig. 9: Predicted kinetic energy from different meshes (left: polyhedron, right: tetrahedron) with similar mesh number on the horizontal axial of the impeller (T=300 mm, 200 rpm).

of the calculation. Fig. 10 shows that either the simulated radial, tangential or axial velocities from the polyhedral mesh of 1.0 million cell number better agrees to the experimental ones than the adaptive tetrahedral mesh of 1.87 million cell number although the adaptive tetrahedral mesh was refined based on the velocity gradient. It approves that the polyhedral mesh can lead to more accurate results which are more closely consistent with the experimental data compared to the adaptive tetrahedral one.

CONCLUSIONS

The performance of various tetrahedral and polyhedral meshes in the single-phase flow simulations of a stirred tank were studied. The CFD simulation results of polyhedral meshes can more closely approximate the experimental findings measured by LDA and PIV method. Converting a tetrahedral mesh into a polyhedral mesh leads to about 66% less mesh cells without missing the simulation accuracy. The polyhedral mesh is found superior than the tetrahedral mesh, partially refine tetrahedral mesh and adaptive tetrahedral mesh in stirred tank simulation since it leads to higher accuracy and higher computational efficiency. The polyhedral mesh also requires less computational time and resources in flow field simulation of a stirred tank to achieve the same accuracy.

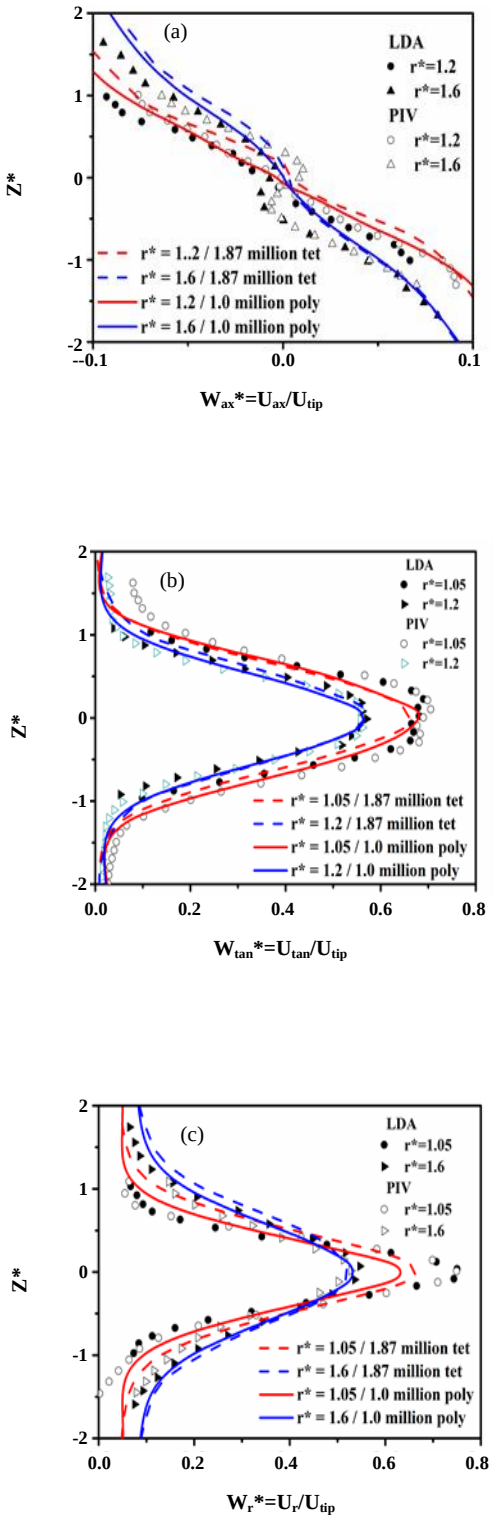

Fig. 10: Axial profiles of non-dimensional average velocity components (a): axial velocity, (b): tangential velocity, (c): radial velocity.

Acknowledgments

The authors would like to acknowledge the financial support provided by the National Key R&D Program of China (2018YFB0605700) and the Provincial Key R&D Program of Shanxi (201603D312003). We would like to express our sincere gratitude to Mr. Giacomo for his help in the English language.

Received : Sep. 2, 2018 ; Accepted :Mar. 21, 2019

REFERENCES

[1] Yang S., Li X., Deng G., Yang C., Mao Z., Application of KHX Impeller in a Low-Shear Stirred Bioreactor, *Chinese J. Chem. Eng.*, **22**(10): 1072-1077(2014).

[2] Cortada-Garcia M., Dore V., Mazzei L., Angeli P., Experimental and CFD Studies of Power Consumption in the Agitation of Highly Viscous Shear Thinning Fluids, *Chem. Eng. Res. Des.*, **119**: 171-182(2017).

[3] Jafari R., Tanguy P.A., Chaouki J., Experimental Investigation on Solid Dispersion, Power Consumption and Scale-Up in Moderate to Dense Solid-Liquid Suspensions, *Chem. Eng. Res. Des.*, **90**(2): 201-212(2012).

[4] Bashiri H., Bertrand F., Chaouki J., Development of A Multiscale Model for The Design and Scale-Up of Gas/Liquid Stirred Tank Reactors, *Chem. Eng. J.*, **297**: 277-294(2016).

[5] Waghmare Y., Falk R., Graham L., Koganti V., Drawdown of Floating Solids in Stirred Tanks: Scale-up Study Using CFD Modeling, *Int. J. Pharmaceut.*, **418**(2): 243-253(2011).

[6] www.CD-adapco.com

[7] Bujalski W., Jaworski Z., Nienow A.W., CFD Study of Homogenization with Dual Rushton Turbines—Comparison with Experimental Results: Part II: The Multiple Reference Frame, *Chem. Eng. Res. Des.*, **80**(1): 97-104(2002).

[8] Vlček P., Kysela B., Jirout T., Fořt I., Large Eddy Simulation of A Pitched Blade Impeller Mixed Vessel Comparison With LDA Measurements, *Chem. Eng. Res. Des.*, **108**: 42-48(2016).

[9] Duan X., Feng X., Yang C., Mao Z.S., Numerical Simulation of Micro-Mixing in Stirred Reactors Using The Engulfment Model Coupled with CFD, *Chem. Eng. Sci.*, **140**: 179-188(2016).

[10] Ng K., Fentiman N.J., Lee K.C., Yianneskis M., Assessment of Sliding Mesh CFD Predictions and LDA Measurements of the Flow in a Tank Stirred by a Rushton Impeller, *Chem. Eng. Res. Des.*, **76**(6): 737-747(1998).

[11] Cortada-Garcia M., Dore V., Mazzei L., Angeli P., Experimental and CFD Studies of Power Consumption in the Agitation of Highly Viscous Shear Thinning Fluids, *Chem. Eng. Res. Des.*, **119**: 171-182(2017).

[12] Xie L., Liu Q., Luo Z., A Multiscale CFD-PBM Coupled Model for the Kinetics and Liquid–Liquid Dispersion Behavior in a Suspension Polymerization Stirred Tank, *Chem. Eng. Res. Des.*, **130**: 1-17(2018).

[13] Gorii M., Bozorgmehry B.R., Kazemeini M., CFD Modeling of Gas-Liquid Hydrodynamicsin a Stirred Tank Reactor, *Iran. J. Chem. Chem. Eng. (IJCCE)*, **26**(2): 85-96(2007).

[14] Spiegel M., Redel T., Zhang Y.J., Struffert T., Hornegger J., Tetrahedral Vs. Polyhedral Mesh Size Evaluation on Flow Velocity and Wall Shear Stress for Cerebral Hemodynamic Simulation, *Comput. Method. Biomec.*, **14**(1): 9-22(2011).

[15] Ben Diedrichs., Aerodynamic Calculations of Crosswind Stability of a High-Speed Train Using Control Volumes of Arbitrary Polyhedral Shape. "*BBAA VI International Colloquium on: Bluff Bodies Aerodynamics & Applications Milano*", Italy, July, 20-24 (2008).

[16] Tritthart M., Gutknecht D., Three-Dimensional Simulation of Free-surface Flows Using Polyhedral Finite Volumes, *Eng. Appl. Comp. Fluid*, **1**(1): 1-14 (2007).

[17] Montante G., Moštěk M., Jahoda M., Magelli F., CFD Simulations and Experimental Validation of Homogenisation Curves and Mixing Time in Stirred Newtonian and Pseudoplastic Liquids, *Chem. Eng. Sci.*, **60**(8-9): 2427-2437(2005).

[18] Jaworski Z., Bujalski W., Otomo N., Nienow A.W., CFD Study of Homogenization with Dual Rushton Turbines - Comparison with Experimental Results Part I: Initial Studies, *Chem. Eng. Res. Des.*, **78**(A3): 327-333(2000).

[19] Zhang Q., Yong Y., Mao Z., Yang C., Zhao C., Experimental Determination and Numerical Simulation of Mixing Time in a Gas-Liquid Stirred Tank, *Chem. Eng. Sci.*, **64**(12): 2926-2933(2009).

[20] Joshi J.B., Nere N.K., Rane C.V., Murthy B.N., Mathpati C.S., Patwardhan A.W., Ranade V.V., CFD Simulation of Stirred Tanks: Comparison of Turbulence Models. Part I: Radial Flow Impellers, *Can. J. Chem. Eng.*, **89**(1): 23-82(2011).

[21] Joshi J.B., Nere N.K., Rane C.V., Murthy B.N., Mathpati C.S., Patwardhan A.W., Ranade V.V., CFD Simulation of Stirred Tanks: Comparison of Turbulence Models (Part II: Axial Flow Impellers), Multiple Impellers and Multiphase dispersions), *Can. J. Chem. Eng.*, **89**(4): 754-816(2011).

[22] Singh H., Fletcher D.F., Nijdam J.J., An Assessment of Different Turbulence Models for Predicting Flow in a Baffled Tank Stirred with a Rushton Turbine, *Chem. Eng. Sci.*, **66**(23): 5976-5988 (2011).

[23] Fathi Roudsari S., Turcotte G., Dhib R., Ein-Mozaffari F., CFD Modeling of the Mixing of Water in Oil Emulsions, *Comput. Chem. Eng.*, **45**(Supplement C): 124-136 (2012).

[24] Chara Z., Kysela B., Konfrst J., Fort I., Experimental Study of Flow in a Tank Stirred by a Rushton Impeller. "AIP Conference Proceedings" 1648, 030031 (2015).

[25] Chara Z., Kysela B., Konfrst J., Fort I., Study of Fluid Flow in Baffled Vessels Stirred by a Rushton Standard Impeller, *Appl. Math. Comput.*, **272**: 614-628 (2016).

[26] www.ansys.com/